Check for updates

Proceedings of ASME Turbo Expo 2010: Power for Land, Sea and Air
GT2010
June 14-18, 2010, Glasgow, UK

GT2010-22279

Effects of design variations of rotor entry cavity geometry on shrouded steam turbine performance

K. G. Barmpalias, A. I. Kalfas[1], R. S. Abhari
LEC, Laboratory for Energy Conversion
Department of Mechanical and Process Engineering
ETH Zurich
Zurich, Switzerland

Toshio Hirano, Naoki Shibukawa
Keihin Product Operations, Toshiba Corporation
230-0045 Yokohama, Japan

Downloaded from https://asmedigitalcollection.asme.org/GT/proceedings-pdf/GT2010/44021/2127/4718401/2127_1.pdf by ETH Zuerich user on 17 October 2019

ABSTRACT

This paper presents an experimental study of the effect of geometry variations of the rotor entry cavity on shrouded steam turbine performance. A series of experiments was carried out where different configurations of the geometry of the entry cavity were tested. Blade geometry and tip clearance remained unaltered for all cases examined. Interactions between cavity and main flow are carefully investigated and their consequences on shrouded steam turbine stage efficiency are examined.

Geometry variations of the entry cavity were installed in a pre-existing 'baseline' case of high efficiency. Five different test cases were examined. For the first two of these cases a ring having a constant width of 2mm and 4mm in radial direction is used. The next two cases employ a non-uniform, wavy insert and for the last case a backwards slanted insert is used that covers most of the inlet to cavity area, maintaining a safety distance of 2mm from the downstream rotor. The cases are divided into two groups, based on the same inlet cavity volume. The first group of three cases has a cavity volume reduction of 14% compared to the baseline case, whereas in the second group two cases are examined which maintain a 28% cavity volume reduction compared to the baseline case. Stage performance and flow field data were acquired and analyzed. Strong interactions between cavity and main flow are observed for all cases, not only at the location where the variations were installed.

An observed effect can also be seen downstream of the rotor affecting the stage performance. Measurements were performed with the use of miniature probes ensuring minimum blockage effects especially within the cavity, both at rotor inlet as well as downstream of the second rotor.

The use of a uniform geometry variation for the inlet rotor cavity in both groups proved to be the best in terms of stage efficiency. Although more complex and non-uniform variations were also used, the simple design of uniform geometry caused the least disturbance in the flow downstream of the 2nd rotor, having at the same time a moderate positive influence at the exit of the 2nd stator.

The use of a constant width insert ring (thickness = 2mm) showed an efficiency gain of at least 0.3% from cases with 14% cavity volume reduction, whereas in the cases with 28% cavity volume reduction the use of a uniform ring of 4mm width produced a marginal efficiency gain of 0.1% at the operational point.

INTRODUCTION

Efficiency losses attributed to leakage flows in shrouded blades account for a substantial part of the total aerodynamic losses in turbomachinery especially in highly loaded turbines with low aspect ratio blades. Potential work that could have been extracted from the rotor blades not only bypasses the

---

[1] Current address: Aristotle University of Thessaloniki, Greece

Copyright © 2010 by ASME

main flow but also causes extensive losses in the tip region of the blades due to changes in the incidence angle.

Egli [1] and Traupel [2] presented respectively theoretical and an experimental approaches in their attempts to quantify mass leakage flow through labyrinth seals. Egli [1] assumed a perfect dissipation of the kinetic energy into heat within the cavity as well as zero initial velocity upstream of the gap. For his empirical correlation, Traupel [2] uses a discharge coefficient based on labyrinth geometry. Mixing of the leakage flow within the inlet cavity recirculation in the interaction with the main flow zone and reinjection at the exit cavity causing negative incidence on the following blade row are processes resulting in efficiency penalties. Wellborn and Okiishi [3] even reported a 1% efficiency reduction for every 1% increase in the clearance to span ratio.

Loss generation in the tip section of the shrouded blades is primarily associated with the mixing process that takes place in the interaction zone between the cavity flow and the main stream. In his review on secondary flows in axial turbines, Langston [4] gave an overview of the work that has been done on secondary flows up to 2001, highlighting the necessity for a better understanding of the associated mechanisms. Earlier, Denton [5] in his work on loss mechanisms in turbomachines more specifically identifies the mixing process during re-entry of the leakage flow as the main entropy creating process causing losses with shrouded blades. Rosic et al. [6] numerically studied the significant influence on the aerodynamics of shroud and inner cavity geometry on turbine performance. He reported the beneficial reduction of cavity length and the insignificant effect of shroud thickness on efficiency. Anker et al. [7] focused on physical effects and losses of leakage and main flow in the rotor and in particular those introduced by the interaction of the main and cavity flows with respect to loss generating mechanisms. He showed the weakening of the upper passage vortex due to the egress of the leakage flow, while the upper secondary passage vortex of the subsequent stator strengthens as the leakage flow is reinjected after the rotor. Hunter and Manwaring [8], and Li et al. [9] talked about leakage flows influencing the downstream flow field even after two blade rows. Research has also been undertaken on the fins of the labyrinth themselves. Vakili et al. [10] studied seal design to examine their influence on leakage characteristics. Having done PIV measurements and computational work, they reported the significance of the fin axial location and angle and the step height on leakage reduction. Flow visualization was also used by Rhode et al. [11], [12] to measure leakage resistance in their water test facility with regard to step shape and height. The interaction of cavity and main flow has also been studied by Peters et al. [13]. They performed steady state measurements together with simulations to report a strongly affected flow field at the subsequent stator at the tip region. Schlienger et al. [14] studied the use of inserts at the exit cavity in an attempt to improve re-entry of the leakage flow, but surprisingly his efficiency results were negative. In another approach, Wallis et al. [15] state that modern sealing arrangements have considerably reduced the leakage fractions to a degree that further improvements can only be achieved by controlling the leakage flow itself, especially the way it re-enters the main flow. By the use of bladelets positioned at the exit cavity onto the shroud they tried to redirect the leakage jet and align it with the main stream. They reported efficiency deficits through poor performance of the bladelets with the main flow now travelling further upwards into the cavity. Pfau et al. [16], [17] systematically investigated cavity flows by analyzing a set of experimental data. They described in detail the dominating kinematic flow feature in the region, the toroidal vortex: a vortex fed with high pressure fluid from the pressure side of the stator blade. The associated fluctuating mass in turn results in negative incidence on the rotor. After having discussed and quantified the secondary flow development and mixing losses they derived design recommendations.

In the case of low solidity turbines, as employed for these measurements, designers need to be aware that the low solidity design approach has already increased secondary losses through higher loading as shown by Song et al.[18]. A substantial part of total losses in turbomachines are associated with leakage flows. As has already been stated, it is not only the mixing processes of in and outflows, but also the potential work of this leakage mass escaping through the labyrinth that could have been extracted by the rotor that help in this direction. In this study, an experimental approach is followed in order to study the influence of the inlet to rotor cavity geometry to the flow field upstream but also downstream of the rotor row. With the use of geometry variations installed at the rotor inlet cavity it is intended to break down the toroidal vortex residing in the cavity responsible for the in and outflows. For all cases studied in this work the cavity volume is kept constant so as to exclude any influence on the leakage mass flow coming from volume changes.

NOMENCLATURE

C_{pt}	pressure coefficient $(P_t - P_{s,exit}) / (P_{t,inlet} - P_{s,exit})$
P	pressure
h	normalized blade span
x, y, z	Cartesian coordinates
z	axial direction

Greek

α	absolute flow yaw angle
γ	flow pitch angle
v	velocity

Abbreviations

Copyright © 2010 by ASME

Downloaded from https://asmedigitalcollection.asme.org/GT/proceedings-pdf/GT2010/44021/2127/4718401/2127_1.pdf by ETH Zuerich user on 17 October 2019

5HP	five hole probe
FRAP	Fast Response Aerodynamic Probe
HS, LS	high solidity stator, low solidity stator
TE, LE	trailing edge, leading edge

Subscripts

R	rotor
S	stator
t	total condition
s	static condition
inlet	turbine inlet condition
exit	turbine exit condition

EXPERIMENTAL METHOD

The research facility

The measurements were performed in the 'LISA' two stage axial research turbine at the Laboratory for Energy Conversion (LEC) of ETH Zurich. The turbine inlet temperature TET is kept constant at 310 K with an accuracy of 0.9 K. A DC generator maintains a constant operating speed of 2750 ±0.5 RPM (±0.02%). The measurement uncertainty of the test facility concerning total to static efficiency of the second stage is ±0.21%. A more detailed description of the test facility is available in Schlienger et al. [19]. The stator blade row configurations differ as shown in Table 1. The first stator is of a high solidity (1.43) design whereas the second stator has a low solidity (1.25). Both stators are designed to have the same exit flow angle and axial chord. The associated operating parameters based on the LS stator are summarized in Table 2. More detailed measurements on the baseline test case can be found in Tashima et al. [20].

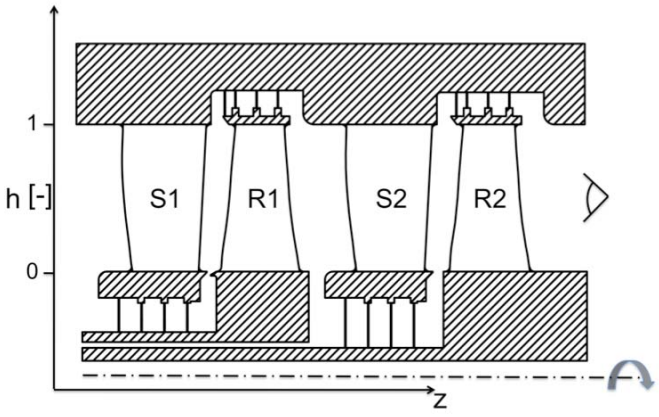

Figure 1: Schematic diagram of the two-stage axial turbine

Parameter	HS stator	LS stator
Blade count Zs	48	36
Axial chord* C_{ax} [mm]	50	50
Chord length* C [mm]	66.3	77.4
Pitch* t [mm]	46.5	62.0
Blade span H [mm]	90	90
Aspect ratio AR = H/C [-]	1.36	1.16
Solidity σ = C/T [-]	1.43	1.25

Table 1: Geometric details of stator blades. (* indicates that dimension is at 50% span)

Rotor speed [RPM]	2750
Overall pressure ratio [-]	1.32
Mass flow [kg/sec]	7.87
Turbine inlet temperature [°C]	37.8
Blade number count stage-1 (stator/rotor)	48/48
Blade number count stage-2 (stator/rotor)	36/48
Tip/hub diameter [mm]	800/620
Flow coefficient (stage-2) [-]	0.3
Loading coefficient (stage-2) [-]	1.0
Mach number (stator/rotor)	0.32/0.1
Reynolds number (rotor)	2×10^5

Table 2. Main parameters of the test case configuration based on the characteristics of the LS stator

Instrumentation

Both steady and unsteady flow field measurements are made. The steady flow field is measured with a 5-hole probe (5HP) with a 0.9 mm head diameter, whereas the unsteady flow field is captured with the use of a 2-sensor Fast Response Aerodynamic Probe (FRAP), which has a 1.8 mm head diameter as shown in Figure 2. For the measurements inside the cavity a miniature 4-hole probe (4HP) was used together with a set of mini FRAP probes of 0.84mm head diameter. Each of the probes is one holed; one that is yaw sensitive and one for the pitch measurement. A full detailed description of the two mini probes can be found in Pfau et al. [21] The FRAP has a measurement bandwidth of 48 kHz. The measured flow parameters and their absolute uncertainties are listed in Table 3. Absolute accuracy of the flow quantities in Table 3 are expressed as % of the calibration range for the angles, % of the dynamic head for pressures and % of the absolute Mach number for the velocity. The use of these probes in the turbine facility 'LISA' has been shown in several publications, including Lenherr et al. [22].

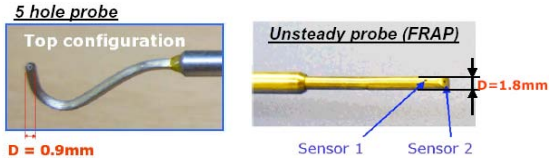

Figure 2: 5HP and FRAP measurement probes

Downloaded from https://asmedigitalcollection.asme.org/GT/proceedings-pdf/GT2010/44021/2127/4718401/2127_1.pdf by ETH Zuerich user on 17 October 2019

Copyright © 2010 by ASME

	α	γ	P_t	P_s	M
FRAP	0.5°	0.7°	1%	1.2%	1%
5HP	0.3°	0.3°	1.8%	2%	0.06%

Table 3: Absolute uncertainties in probe measurements for a calibration range of yaw ±30 pitch ±20 and for a Mach number of 0.3. (pressure % of the dynamic head, Mach number % of the absolute Mach number)

Probe measurements were made at the rotor exit and downstream of the LS stator. Measurements at the stator exit were made 6mm downstream of the stator at h=1 while inside the cavity. Therefore, the measurement plane is located at $0.224C_{ax}$ downstream of the 2nd stator's trailing edge at midspan. The measurement grids consist of 48 points and 61 points evenly distributed in the radial and circumferential directions respectively. The circumferential traverse was conducted over three LS stator pitches. Data are sampled at 200 kHz, which corresponds to 92 samples per blade passing period. A phase-lock data averaging procedure is performed over 90 rotor revolutions.

Inlet cavity

This research turbine has a sealing configuration of 4 seals with a gap of 0.4mm corresponding to 0.44% of the blade span. The inlet cavity under investigation is the one illustrated in Figure 3. It has a volume of $5x10^5$ mm^3.

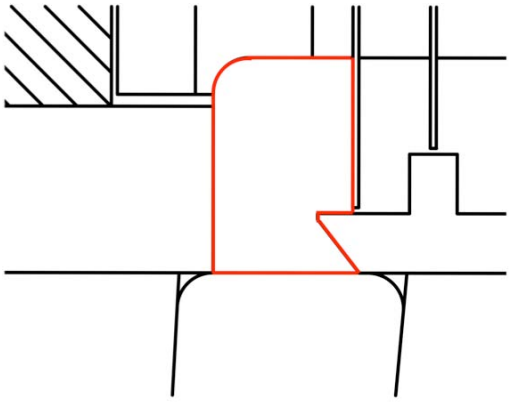

Figure 3: Illustration of the inlet cavity

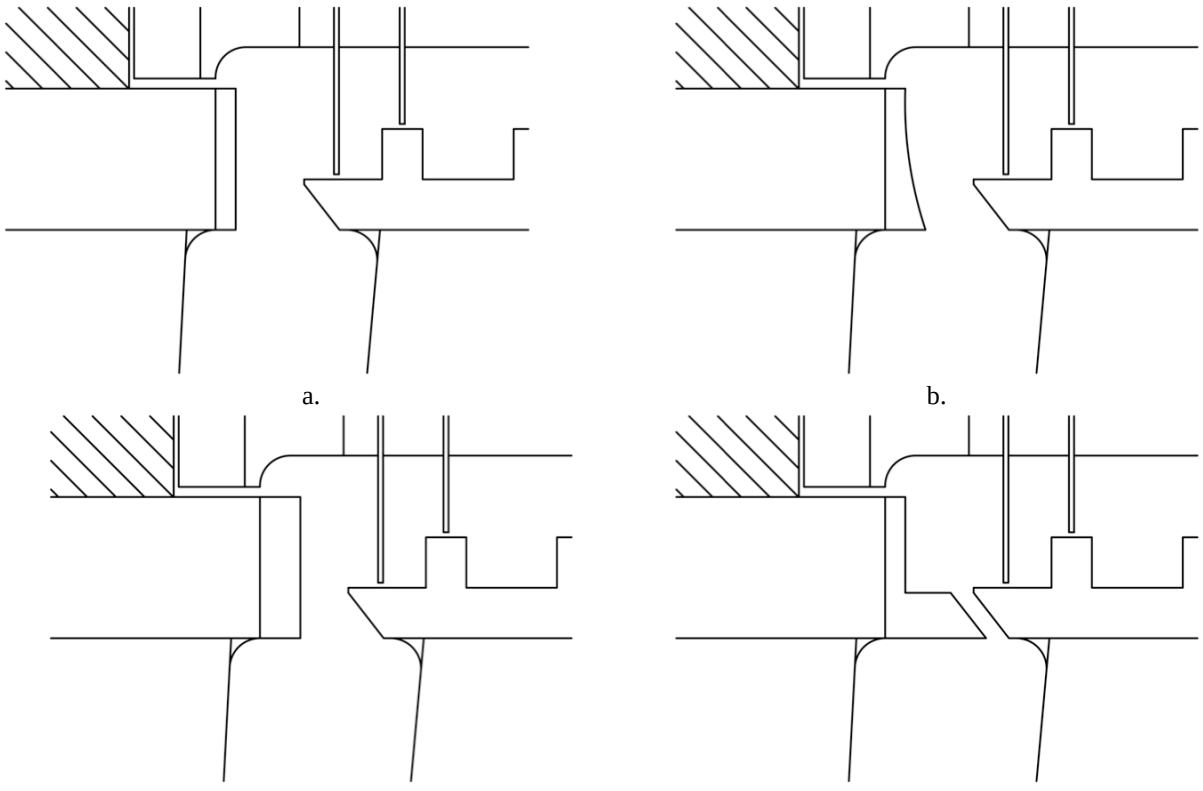

Figure 4: a. uniform 2mm insert, b. non-uniform insert, c. uniform 4mm insert and d. slanted insert; rotor inlet cavity meridional cut

Downloaded from https://asmedigitalcollection.asme.org/GT/proceedings-pdf/GT2010/44021/2127/4718401/2127_1.pdf by ETH Zuerich user on 17 October 2019

Copyright © 2010 by ASME

The dimensions are 12mm x 18mm with a minimum distance during operation of 8mm between the rotor shroud and stator. Five different configurations were tested divided in 2 groups. In each group, the cavity volume is kept constant to eliminate any influence originating from cavity volume variations. All cases stem from the baseline case, where with the use of inserts there is a cavity volume reduction of 14% and 28% for the 1st and 2nd group respectively compared to the baseline case. In the first group 3 cases were considered.

First, a uniform radial direction 2mm ring is attached to the stator's side of the cavity as shown in Figure 4a. In the other two cases, two different non-uniform rings are tested, varying from a minimum of 2mm to 4mm in width, as seen in Figure 5a. Both rings have 36 bumps, the same as the number of stator blades and they can be circumferentially clocked with respect to the stator's trailing edge as in Figure 5b. The design of the bumps is intended to hinder the high pressure fluid stemming from the pressure side of the blade from entering the cavity and at the same time to allow low pressure fluid to enter. Lower pressure fluid inside the cavity will finally result in a lower pressure difference between inlet and exit cavities and therefore less leakage flow escaping through the labyrinth.

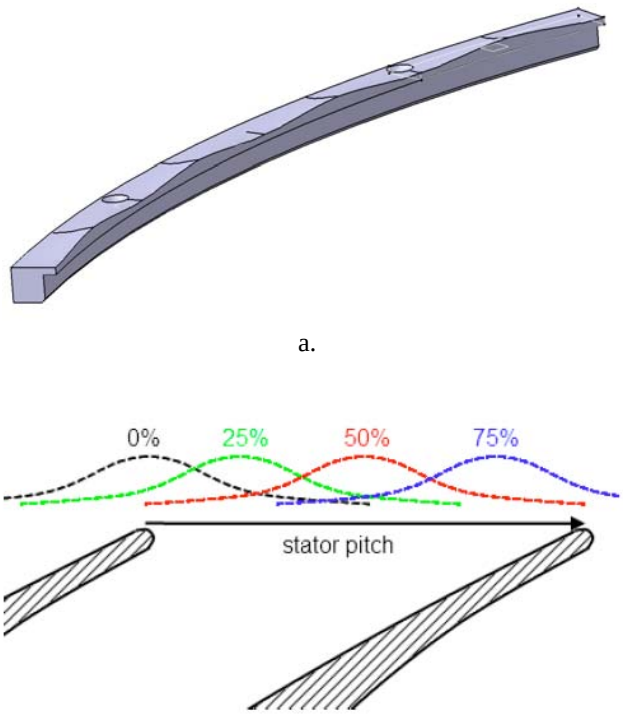

a.

b.

Figure 5: a. CAD design of non-uniform ring and b. clocking positions of the non-uniform ring

In Figure 6 a comparative schematic of the two designs is illustrated at span height h=1, at the cavity inlet. The second design of the non-uniform insert will offer a wider blockage, expected to prevent even more the high pressure fluid from entering the cavity. The second ring is clocked and tested in 3 circumferential positions. The cavity volume reduction is again of the order of 14%, allowing for a direct comparison with the other cases of this group. The first non-uniform insert was tested in two circumferentially clocked positions, at 25% and 50%. The second ring was tested in the circumferential clocking positions at 25%, 50% and 75% of the stator pitch compared to the stator's trailing edge.

The second group consists of two test cases; one with a uniform 4mm ring as shown in Figure 4c and another where a slanted insert is used as in Figure 4d. This insert covers 10mm of the cavity inlet area at h=1, corresponding to 83% of the available area and is chamfered backwards maintaining a safety distance of 2mm from the shroud's rotor up to h=1.06.

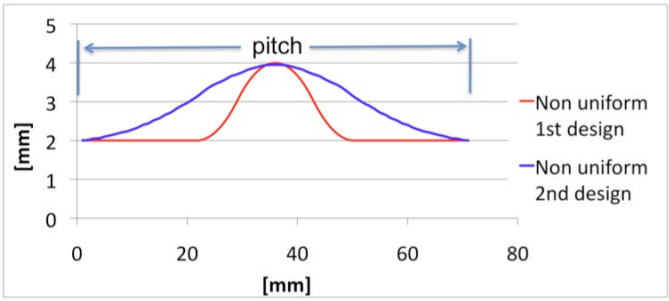

Figure 6: non-uniform designs at h=1

Fluid originating from the pressure side of the stator blade though at higher pressure moves upwards inside the cavity while fluid exits the inlet cavity within the low momentum fluid of the stator wake. The main objective of all cases under consideration is the control of this radially moving flow in and out of the inlet cavity.

This study aims to examine the secondary flow effects dominating the interaction zone between the main and cavity flows through the use of inserts in the inlet cavity. In a further step, these changes in inlet cavity geometry are associated with efficiency changes.

RESULTS AND DISCUSSION

Cavity volume reduction of 14%

Initially the cases where the use of cavity inserts lead to a 14% cavity volume reduction compared to the baseline case are considered. Figures 4a and 4b show a schematic of these cases. In Figure 7a the time-averaged total pressure loss coefficient is presented along with the mass averaged value in Figure 7b. for the first design of the non-uniform ring circumferentially clocked at 25% and 50% of the stator pitch together with the uniform 2mm case at the second stator exit. Measurements were made up to 85% of the blade span due to probe access restrictions. The plot covers 30° and three stator pitches. Dashed lines represent the upstream stator's trailing

Copyright © 2010 by ASME

Downloaded from https://asmedigitalcollection.asme.org/GT/proceedings-pdf/GT2010/44021/2127/4718401/2127_1.pdf by ETH Zuerich user on 17 October 2019

edge. The extensive losses in the vicinity of the blade's tip area are clearly identified for both the cases that the non-uniform ring is used. In particular in the case when the ring is circumferentially clocked at 25% of the stator's pitch, losses cover the last 10% of the span. Losses on the tip area of the 50% clocking position appeared to be considerably less though covering the 95% - 100% of the blade span. As the bump has circumferentially positioned itself towards the pressure side of the blade it is now located above the high pressure fluid. Therefore it prevents the latter from entering the cavity. Flow improves dramatically when a uniform 2mm ring is installed. The use of the non-uniform ring pushes down radially the position of the upper passage vortex compared to the uniform case.

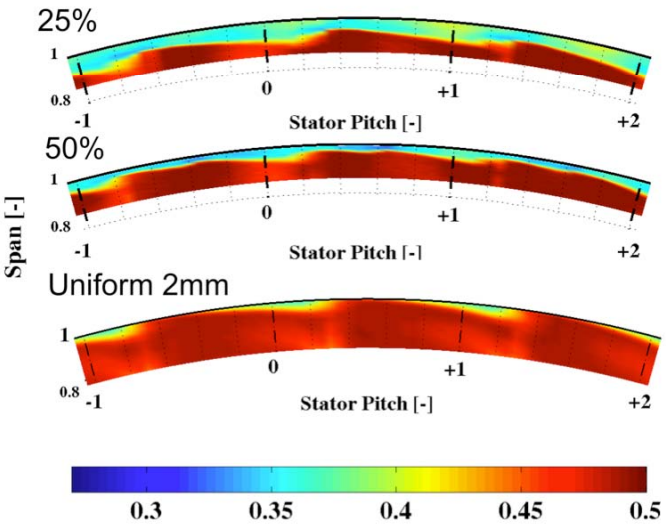

a.

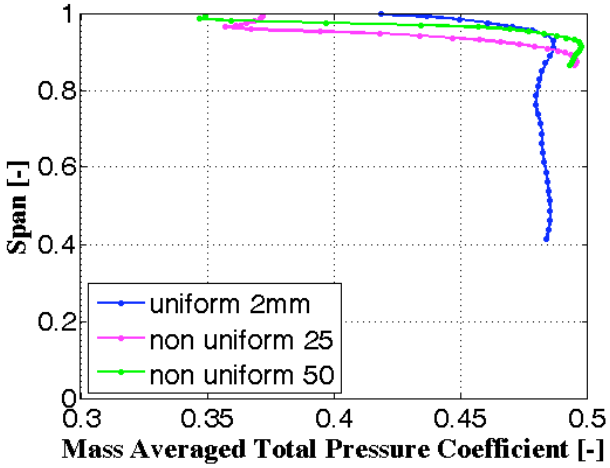

b.

Figure 7: a.Time-averaged total to static pressure coefficient and b. mass averaged total to static pressure coefficient. Comparison of the cases: non-uniform 25%, non-uniform 50% of the first design and uniform 2mm. Stator exit

This displacement of the vortex away from the casing is itself loss generating. The upper passage vortex expands and more mass is now involved in the circular motion. Additionally, for the 25% clocking position a downward flow movement can be identified directly above the upper passage vortex, as shown in Figure 8. It is fed by fluid exiting the cavity. The latter combined with the radially upward fluid movement on the pressure side of the blade gives rise to a vortical structure in the interaction zone between the main and cavity flows. Low values of total pressure loss coefficient are attributed to this additional mixing now present for the 25% clocking position. Moreover, both non-uniform cases experience a strong upward fluid motion on the pressure side of the blade that is intensified as we approach the cavity inlet. More fluid enters the cavity for both non-uniform cases and apparently exits at another plane when compared to the uniform case.

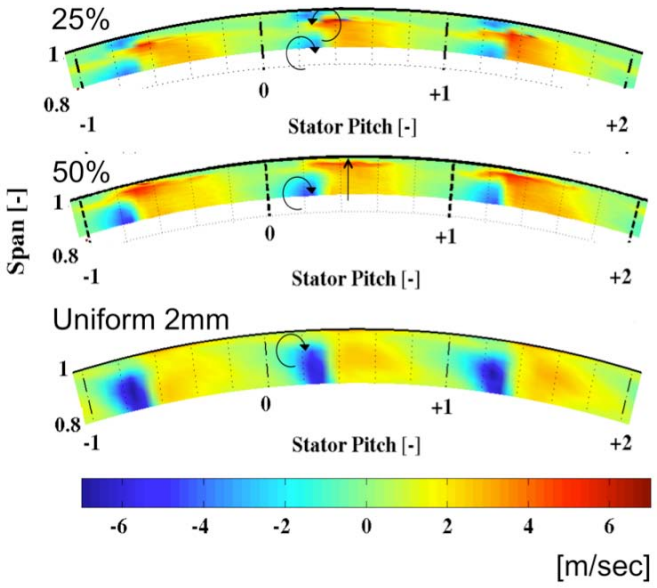

Figure 8: Time-averaged radial velocity. Comparison between the cases: non-uniform 25%, non-uniform 50% of the first design and uniform 2mm. Stator exit

Figure 9a presents the time averaged total to static pressure coefficient along with the mass-averaged value in Figure 9b for the second design of the non-uniform ring clocked in 3 positions compared to the uniform 2mm. Measurements took place at up to 40% of the blade span and inside the cavity. At the tip region, specifically at 95%, inside the main flow the difference between the cases can be identified. The uniform 2mm and the non-uniform cases clocked at 25% are identical. When the ring is clocked at 50% and 75% losses appear to gradually reduce.

As the insert is clocked from 25% towards 75% or from suction to pressure side the bump circumferentially moves and positions itself above the high pressure fluid. The latter finds

Downloaded from https://asmedigitalcollection.asme.org/GT/proceedings-pdf/GT2010/44021/2127/4718401/2127_1.pdf by ETH Zuerich user on 17 October 2019

Copyright © 2010 by ASME

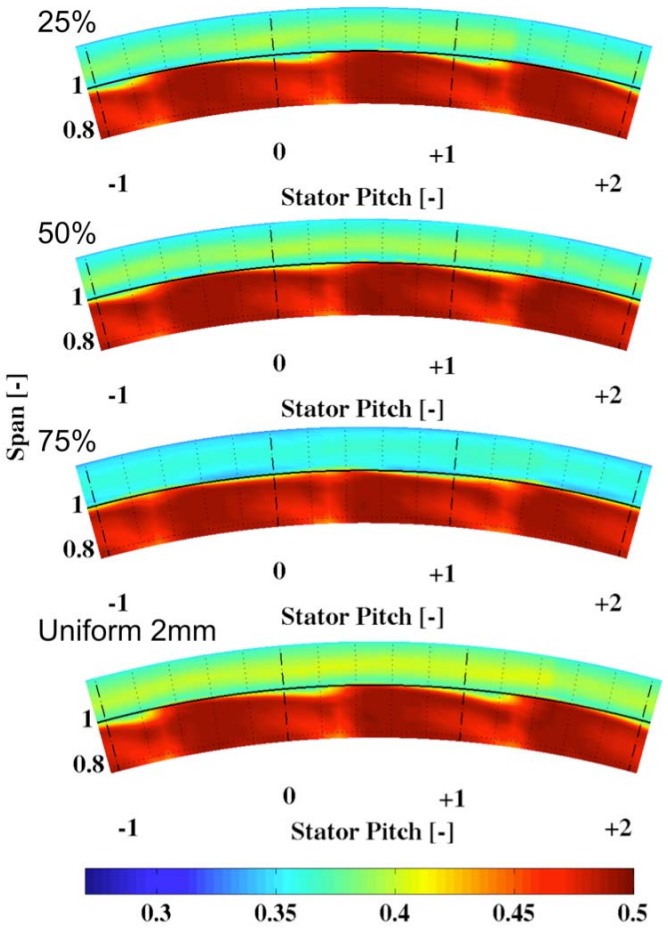

a.

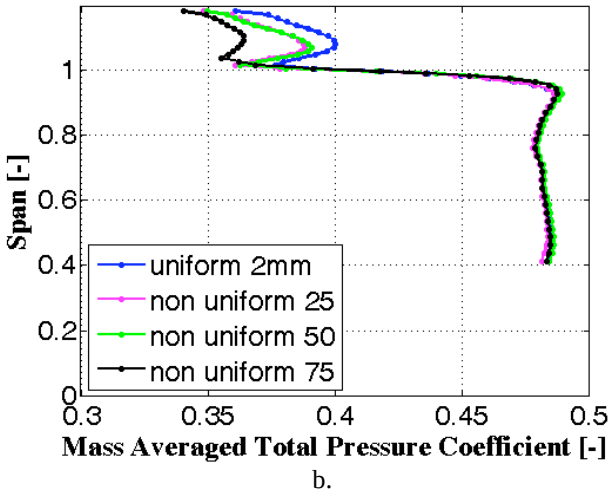

b.

Figure 9: a. Time-averaged total to static pressure coefficient b. mass averaged total to static pressure coefficient; comparison between the cases: non-uniform clocked at positions 25%, 50% and 75% of the second design and uniform 2mm. Stator exit

the way into the cavity more difficult because of the wider bump. Changes in the inlet cavity geometry do not seem to affect the main flow field below 95%. The identical flow field in the main flow between the cases of uniform 2mm and 25% clocking positions implies that when the flow impinges on the upper wall casing it does so when the non-uniform ring has a width of 2mm.

While the main flow field is identical, inside the cavity the influence of the non-uniform design can be observed. Total pressure is lower for all 3 clocking positions compared to the uniform case. The pressure for the 75% clocking position is lowest. This is expected as in the 75% clocking position the high pressure fluid is prevented from entering the cavity. It seems that lower pressure fluid enters the cavity from to the side of the bump.

Losses were expected to be higher at the tip region owing to the overall increased length of the non-uniform insert compared to the uniform 2mm. The extended width should have provided the necessary space for the new boundary layer to develop, a process known to be loss generating. However, this was not experimentally observed. For the clocking positions of 50% and 75% the losses attributed to the upper casing boundary layer are reduced, whereas the 25% clocking position resembles the uniform 2mm case. Up to the trailing edge of the stator blade the new boundary layer generation mechanism is active. Once this is released from the blade passage the skewed boundary layer is subjected only to the main swirling flow. This causes the skewed boundary layer to straighten up. The longer length on the endwall provides the necessary space for the boundary layer development. As a result, a less skewed boundary layer appears at the sampling station.

Another mechanism that also contributes to the reduction of losses in that area is the increased suction inside the cavity though the inlet area for the non-uniform cases which is now less with the pressure drop across the rotor acting as a driving force to remain the same. The new boundary layer forming at the casing is sucked into the cavity. The low momentum boundary layer originating from the upper casing fills the cavity instead of the high energy fluid from the pressure side of the blade. When examining the absolute yaw angle at stator exit, Figure 10 shows that a difference from 95% - 100% of the blade span can be identified. While the uniform 2mm case is identical in the main flow with the non-uniform clocked at 25% as already mentioned, the other 2 clocking positions differ.

The overturning part of the upper passage vortex appears to be elongated, reaching 80^o and 82^o respectively for the 50% and 75% cases. Since the underturning part remains unaltered, the vortex is of the same size. The newly formed boundary layer of the upper wall casing is the one causing the elongation of the overturning leg. The 75% clocking position has the smallest boundary layer height forming at larger angles and while within the interaction zone between the two flows at the tip region the flow experiences a 10^o jump from main flow to cavity. Shear stresses in that region are high which is a loss-

Downloaded from https://asmedigitalcollection.asme.org/GT/proceedings-pdf/GT2010/44021/2127/4718401/2127_1.pdf by ETH Zuerich user on 17 October 2019

Copyright © 2010 by ASME

generating mechanism. Therefore, when the non-uniform ring is clocked at 75% of the stator pitch the lowest stresses are experienced since the smallest jump exists. A circumferential mass flux averaging on that measurement plane as shown in Figure 11 and with h=0.994 reveals that all cases examined experience radial mass flux variations.

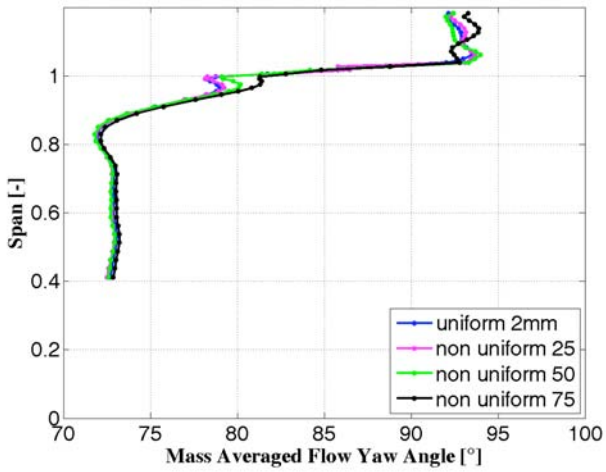

Figure 10: Mass-averaged yaw angle. Comparison between the cases: non-uniform clocked at positions 25%, 50% and 75% of the second design and uniform 2mm. Stator exit

Oscillations on the balance of in and outflows owing to the potential rotor flow field are similar for all cases. Specifically, the uniform 2mm and 25% clocking position follow the same trend, and the 50% and 75% clocking positions experience almost identical oscillations.

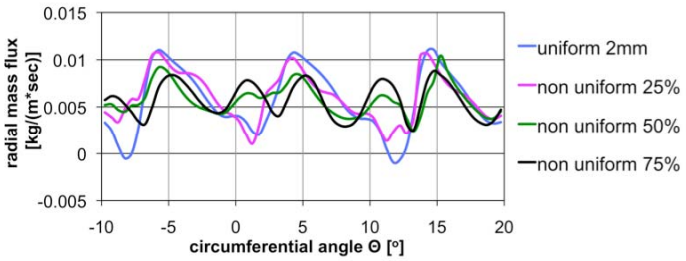

Figure 11: Radial mass flux at h=0.994. Stator exit

Nevertheless, the mass flux entering the cavity at this measurement plane is 7% less for the uniform 2mm case compared to the 25% clocking position, and respectively the 3% and 2% from the 50% and 75% clocking positions. This reveals that both the stator and the rotor are influencing cavity flow mechanisms. The stator dictates the amount of mass flux that finally enters the cavity, but the rotor in turn regulates the in and outflow oscillation.

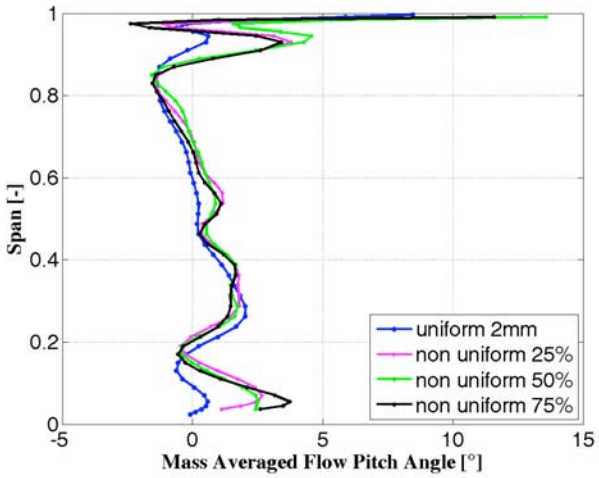

Figure 12: Mass-averaged pitch angle: comparison between the cases with 14% cavity volume reduction. Rotor exit

Figure 12 shows that while the relative yaw angle at the rotor exit is identical for all 4 cases examined, considerable differences are present for the pitch angle. The upper passage vortex is pronounced for all 3 non-uniform cases. There is a 4^o offset between the uniform 2mm case and the non-uniform cases. The 50% clocking position shows the worst efficiency. The upper passage vortex for the uniform 2mm case is confined relative to the other cases, with its limits extending close to 0^o. Moreover, the image we get of the reduced secondary flow non-uniformities across the span for the uniform 2mm case is unexpected, especially in the mid-span.

With respect to the efficiency changes, all non-uniform cases present deficits relative to the uniform 2mm as shown in Figure 13. Although the flow field for the non-uniform cases especially when clocked at 75% of the stator pitch appears to be better in terms of losses being generated at the tip region at the exit of the stator, secondary flows developing at the exit of the rotor finally create a deficit in overall stage efficiency.

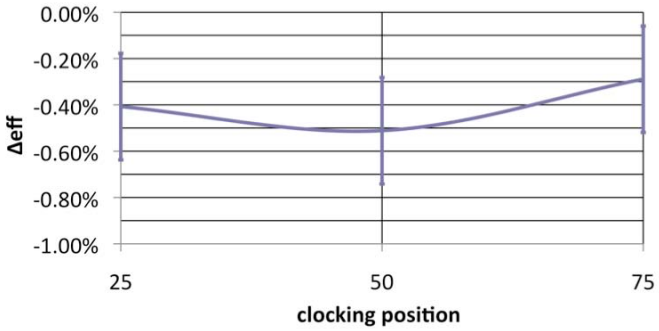

Figure 13: Total to static efficiency changes of the 2nd design of non-uniform cases relative to the uniform 2mm at operating point

Downloaded from https://asmedigitalcollection.asme.org/GT/proceedings-pdf/GT2010/44021/2127/4718401/2127_1.pdf by ETH Zuerich user on 17 October 2019

Copyright © 2010 by ASME

When the non-uniform ring is clocked at 75% of the pitch this brings the bump where the greatest width is close to the pressure side of the blade. The part of the ring with a 2mm width is located on the suction side of the blade at 25% of the pitch. Considering the fact that the flow at the tip region has a yaw angle of 75^o to 80^o, the suction side of the wake is the one approaching the cavity inlet where there is the smallest width. The pressure side of the wake following the flow path impinges on the ring when the width is 4mm. Therefore it is more difficult for the high pressure fluid to enter the cavity. The resemblance between the uniform 2mm and non-uniform cases clocked at 25% is owed to the clocking position of the ring that now enables easier access of the cavity inlet area to the pressure side of the wake.

Cavity volume reduction of 28%

In this group two test cases are examined as shown in Figures 4c and 4d. They both have a reduction of 28% in the cavity volume. In the first case, a 4mm ring which is uniform in the radial direction is used, as shown in Figure 4c. In the other case, a ring that covers 83% of the cavity inlet area is tested. This ring has a backwards slanting face on the rotor side of the cavity maintaining a safety distance of 2mm from the rotating rotor shroud as illustrated in Figure 4d. The use of this ring prohibits the direct radial access from cavity to main flow. Fluid cannot migrate in a radial direction and enter the cavity radially upwards. This configuration does not allow for measurements in this plane, the stator exit. Measurements were made up to h=1.1 of the span.

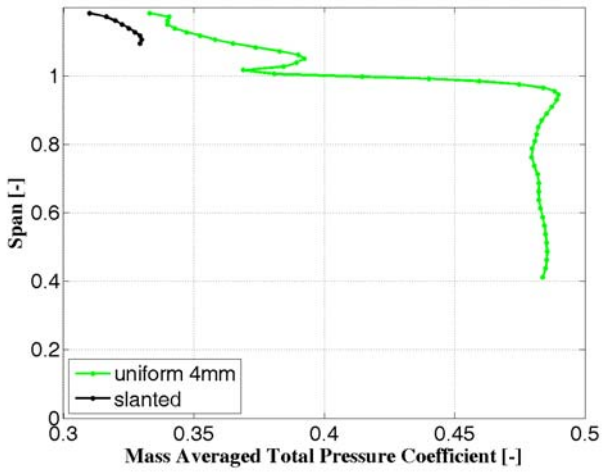

Figure 14: Mass-averaged total pressure coefficient: comparison between the cases with 28% cavity volume reduction. Stator exit

The mass-averaged total pressure coefficient at the stator exit shown in Figure 14 reveals the lower pressure levels for the slanted case inside the cavity. The non-radial accessibility acts as a vane lowering the pressure inside the cavity by strangling the flow. The strangling procedure itself is loss producing.

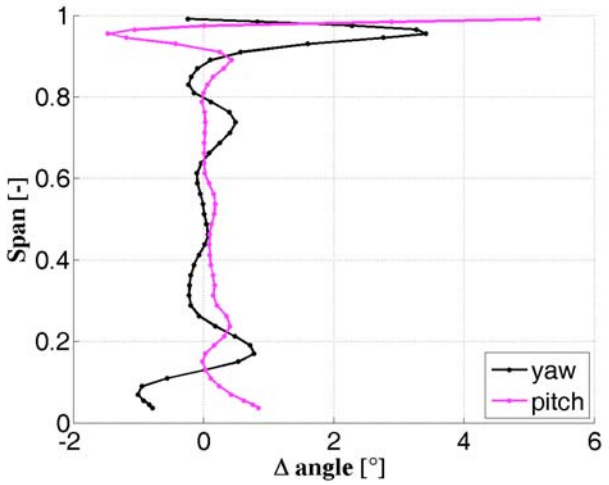

Figure 15: mass-averaged pitch and yaw angle difference for the cases with 28% cavity volume reduction. Uniform 4mm - slanted. Rotor exit.

The difference between the uniform 4mm case and the slanted one with regard to the yaw and pitch angle distribution along the span at the rotor exit is plotted in Figure 15.

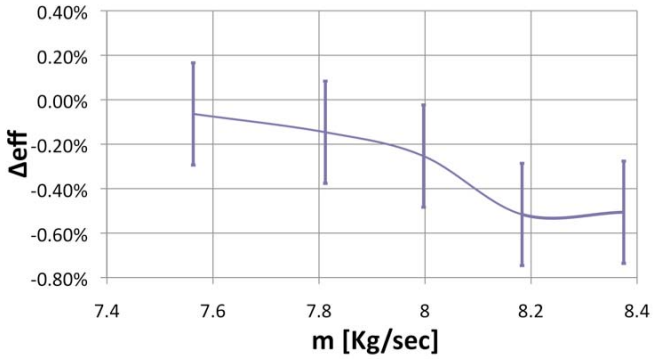

Figure 16: Total to static efficiency changes between the cases with cavity volume reduction of 28%. Slanted - Uniform 4mm case.

While there is no difference on the main core flow, as expected the upper 10% of the blade experiences differences between the 2 cases. The uniform 4mm case shows greater yaw angles with a peak of 3.5^o at 95% blade span. On the

Copyright © 2010 by ASME

Downloaded from https://asmedigitalcollection.asme.org/GT/proceedings-pdf/GT2010/44021/2127/4718401/2127_1.pdf by ETH Zuerich user on 17 October 2019

same span position, the pitch angle for the uniform 4mm case is lower by -1.5^o compared to the slanted case. The uniform 4mm test case experiences greater turning of the flow, but at the same time in the radial direction less negative fluid migration.

Nevertheless, when examining the efficiency changes between the 2 cases in Figure 16, there is a stage efficiency deficit for the slanted case of 0.1% at the operational point.

CONCLUSIONS

This paper presents an experimental investigation performed at the inlet to the rotor cavity of a 2-stage axial steam turbine. A number of modifications of the inlet cavity geometry were tested while maintaining the same cavity volume. Two sets of inserts were tested, having cavity volume reductions of 14% and 28% with respect to the baseline case. The impact of these inserts on stage efficiency through the handling of leakage flows was investigated.

The use of simple geometric variations on the inlet rotor cavity proved to have beneficial effects on turbine stage efficiency compared to all other cases examined. The uniform 2mm insert has efficiency gains compared to all non-uniform cases of at least 0.3%. On the other hand, the uniform 4mm insert showed only marginal benefits as 0.1% is within the efficiency accuracy measurement range of the test turbine.

Although the uniform 2mm design did not improve the flow field at the inlet cavity in terms of in and outflows at the interaction zone, it is the reduction in secondary non-uniformities at the rotor exit that gave the advantage of better efficiency. The non-uniform clocking positions of 50% and 75% for the second design reduced the radial fluid migration but the design had a negative impact on the rotor since the upper passage vortex grew in size compared to the uniform 2mm case.

At the rotor exit the uniform 4mm test case showed greater flow turning at the tip region where the boundary layer develops, but less fluid migration. The efficiency deficit of the slanted case points in the direction of a worsened flow field at the rotor inlet.

This study suggests that the design of cavity geometry is not trivial. It plays a crucial role affecting the flow field at the zone of interaction between the cavity and the main flow, but we can also see prints of these changes downstream of the next blade row.

ACKNOWLEDGMENTS

The authors would like to gratefully acknowledge the contribution of Mr. Tsuguhisa Tashima, Mr. Tadashi Tanuma, Mr. Takashi Sasaki and Mr. Hideo Nomoto in the design and development of these test cases. The permission of the Toshiba Corporation to publish these data is also acknowledged. Special thanks are owed to Mr. H. Suter and Mr. C. Reshef for their technical support throughout the measurement campaign.

REFERENCES

[1] Egli, A., 1935, “The Leakage of Steam through Labyrinth Seals”. Transactions of the ASME, 57, pp. 115-122

[2] Traupel, W., 1973. Thermische Turbomaschinen. Springer-Verlang, Berlin

[3] Wellborn S. R., Okiishi, T. H., 1999, “The Influence of Shrouded Stator Cavity Flows on Multistage Compressor Performance,” ASME J. of Turbomachinery, Vol. 121 / 486, July 1999.

[4] Langston, L. S., 2001, “Secondary Flows in Axial Turbines – a Review,” Annals New York Academy of Sciences

[5] Denton, J. D., 1993, “Loss Mechanisms in Turbomachines,” The 1993 IGTI Scholar Lecture, ASME J. of Turbomachinery, Vol. 115, pp. 621-656.

[6] Rosic, B., Denton, J. D., Curtis, E. M., 2007, “The Influence of Shroud and Cavity Geometry on Turbine Performance – An Experimental and Computational Study, Part 1: Shroud Geometry,” ASME GT2007 – 27769.

[7] Anker, J. E., Mayer J. F., Casey M. V., 2005, “The Impact of Rotor Labyrinth Seal Leakage Flow on the Loss Generation in an Axial Turbine,” Proc. IMechE Vol. 219 Part A: J. Power and Energy

[8] Hunter, S. D., Manwaring, S. R., 2000, “Endwall Cavity Flow Effects on Gas Path Aerodynamics in an Axial Flow Turbine: Part 1- Experimental and Numerical Investigation,” ASME 2000-GT-651

[9] Li, J., Yan, X., LV, Q., Xie, Y., Feng Z., “The Effect of the Shrouded Rotor Blade Tip Leakage Flow on the Aerodynamic Performance of a One and Half Turbine Stage,”.

[10] Vakili, A. D., Meganathan, A. J., Michaud, M., Radhakrishnan, S., 2005, “An Experimental and Numerical Study of Labyrinth Seal Flow,” ASME GT2005-68224

[11] Rhode, D. L., Johnson, J. W., Broussard, D. H., 1997, “Flow Visualization and Leakage Measurements of Stepped Seals: Part 1 – Annular Groove,” ASME J. of Turbomachinery, Vol. 119 / 839, April 1997.

[12] Rhode, D. L., Johnson, J. W., Broussard, D. H., 1997, “Flow Visualization and Leakage Measurements of Stepped Seals: Part 2 – Sloping Surfaces,” ASME J. of Turbomachinery, Vol. 119 / 844, April 1997.

[13] Peters, P., Giboni, A., Menter, J. R., Pfost, H., Wolter, K., 2005, “Unsteady Interaction of Labyrinth Seal Leakage Flow and Downstream Stator Flow in a Shrouded 1.5 Stage Axial Turbine,” ASME GT2005-68065

[14] Schlienger, J., Kalfas, A. I., Abhari, R. S., 2004, “Vortex-Wake-Blade Interaction in a Shrouded Axial Turbine,” ASME GT-2004-53915

[15] Wallis A. M., Denton J. D., Demargne A. A. J., “The Control of Shroud Leakage Flows to Reduce Aerodynamic Losses in a Low Aspect Ratio Shrouded Axial Flow Turbine,” ASME J. of Turbomachinery, Vol. 123 / 335, April 2001.

Downloaded from https://asmedigitalcollection.asme.org/GT/proceedings-pdf/GT2010/44021/2127/4718401/2127_1.pdf by ETH Zuerich user on 17 October 2019

Copyright © 2010 by ASME

[16] Pfau, A., Schlienger, J., Kalfas, A. I., Abhari, R. S., 2003, “Unsteady Flow Interactions within the Inlet Cavity of a Turbine Rotor Tip Labyrinth Seal,” ASME GT2003-38271

[17] Pfau, A., Kalfas, A. I., Abhari, R. S., 2003, “Making use of Labyrinth Interaction Flow,” ASME GT2004-53797

[18] Song, Bo., Wing, F. Ng., Controneo, J. A., Hofer, D. C., Siden, G., 2004, “Aerodynamic Design and Testing of Three Low Solidity Steam Turbine Nozzle Cascades,” ASME GT2004-53329

[19] Schlienger, J., Pfau, A., Kalfas, A. I., Abhari, R. S., 2003, “Effects of Labyrinth Seal Variation on Multistage Axial Turbine Flow,” ASME GT2003-38270

[20] Tashima, T., Sasaki, T., Kalfas, A. I., Abhari, R. S., 2007, “Blade Loading Influence on Unsteady Flow Interactions in Axial Steam Turbines,” ASME GT2007-27452

[21] Pfau, A., Schlienger, J., Kalfas, A. I., Abhari, R. S., 2003, “Unsteady, 3-Dimensional Flow Measurement using a Miniature Virtual 4-sensor Fast Response Aerodynamic Probe (FRAP),” ASME GT2003-38128

[22] Lenherr, C., Kalfas, A. I., Abhari, R. S., 2007, “A Flow Adaptive Aerodynamic Probe Concept For Turbomachinery,” Meas. Sci. Technol. Vol. 18, pp. 2599-2608

Downloaded from https://asmedigitalcollection.asme.org/GT/proceedings-pdf/GT2010/44021/2127/4718401/2127_1.pdf by ETH Zuerich user on 17 October 2019

Copyright © 2010 by ASME